Supporting Information

Magnetic-controlled dandelion-like nanocatalytic swarm for targeted biofilm elimination

Yanjie Huang#, Dong Liu#, Ruirui Guo, Bin Wang, Zhengzuo Liu, Yijia Guo, Jian Dong, Yuan Lu**

Yanjie Huang, Ruirui Guo, Prof. Jian Dong

Tianjin Industrial Microbiology Key Laboratory, College of Biotechnology, Tianjin University of Science and Technology, Tianjin 300457, China

Dong Liu, Bin Wang, Zhengzuo Liu, Yijia Guo, Prof. Yuan Lu

Key Laboratory of Industrial Biocatalysis, Ministry of Education, Department of Chemical Engineering, Tsinghua University, Beijing 100084, China.

*Corresponding authors. Email: yuanlu@tsinghua.edu.cn (Y. Lu),

dongjian@tust.edu.cn (J. Dong)

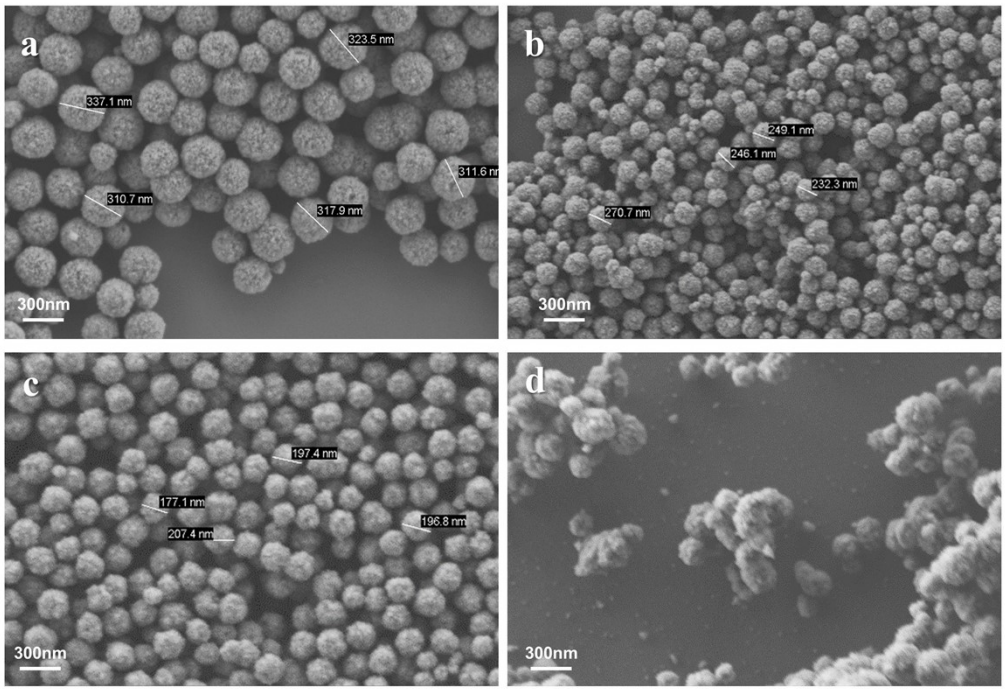

Figure S1. SEM images of the Fe_3O_4 magnetite particles prepared by the solvothermal reaction with 0.3 g of Na_3Cit, 6.0 g of NaAc and different $FeCl_3 \cdot 6H_2O$ concentration of a) 2.2 g, b) 3.25 g, c) 5 g, d) 7 g in 100 mL of ethylene glycol at 200 °C for 10 h.

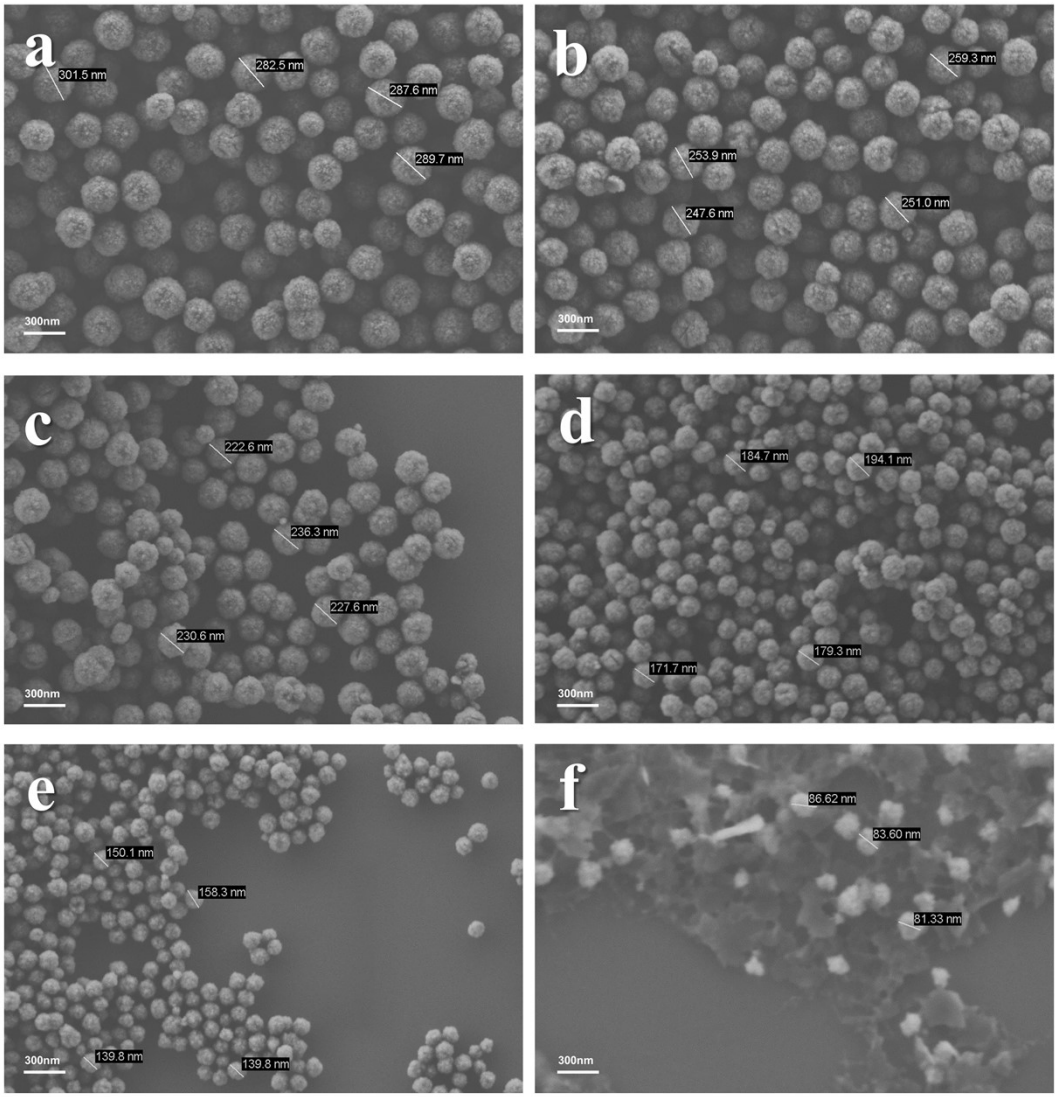

Figure S2. SEM images of the Fe_3O_4 magnetite particles prepared by the solvothermal reaction with 3.25 g of $FeCl_3$•$6H_2O$, 6.0g of NaAc and different Na_3Cit concentration of a) 0.05 g, b) 0.25 g, c) 0.5 g, d) 0.75 g, e) 1.0 g, f) 1.5 g in 100 mL of ethylene glycol at 200 °C for 10 h. With the increase of Na_3Cit mass, the diameter of Fe_3O_4 decreases.

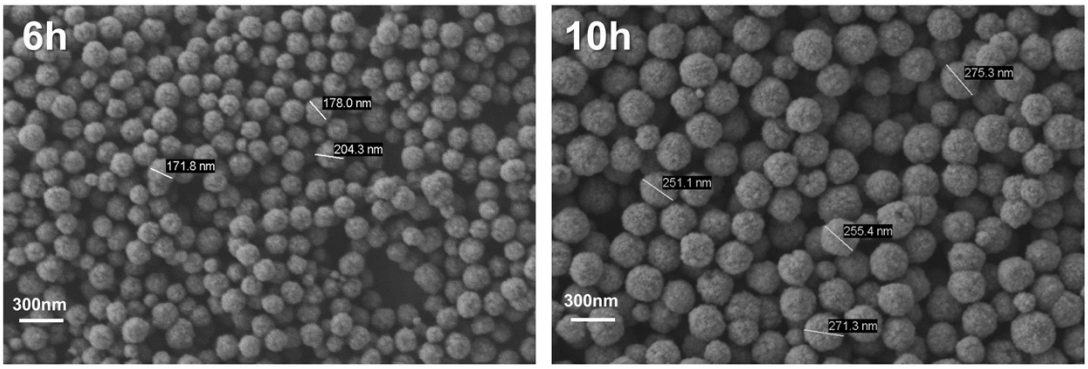

Figure S3. SEM images of the Fe_3O_4 magnetite particles prepared by the solvothermal reaction with 3.25 g of $FeCl_3$•$6H_2O$, 0.30 g of Na_3Cit and 6.0 g of NaAc in 100 mL of ethylene glycol at 200 °C for different reaction time

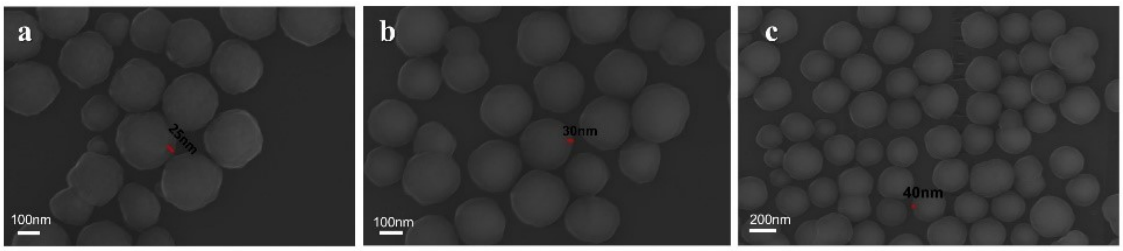

Figure S4. Fe_3O_4@nSiO_2 SEM images with different thicknesses were prepared by adjusting the amount of TEOS.

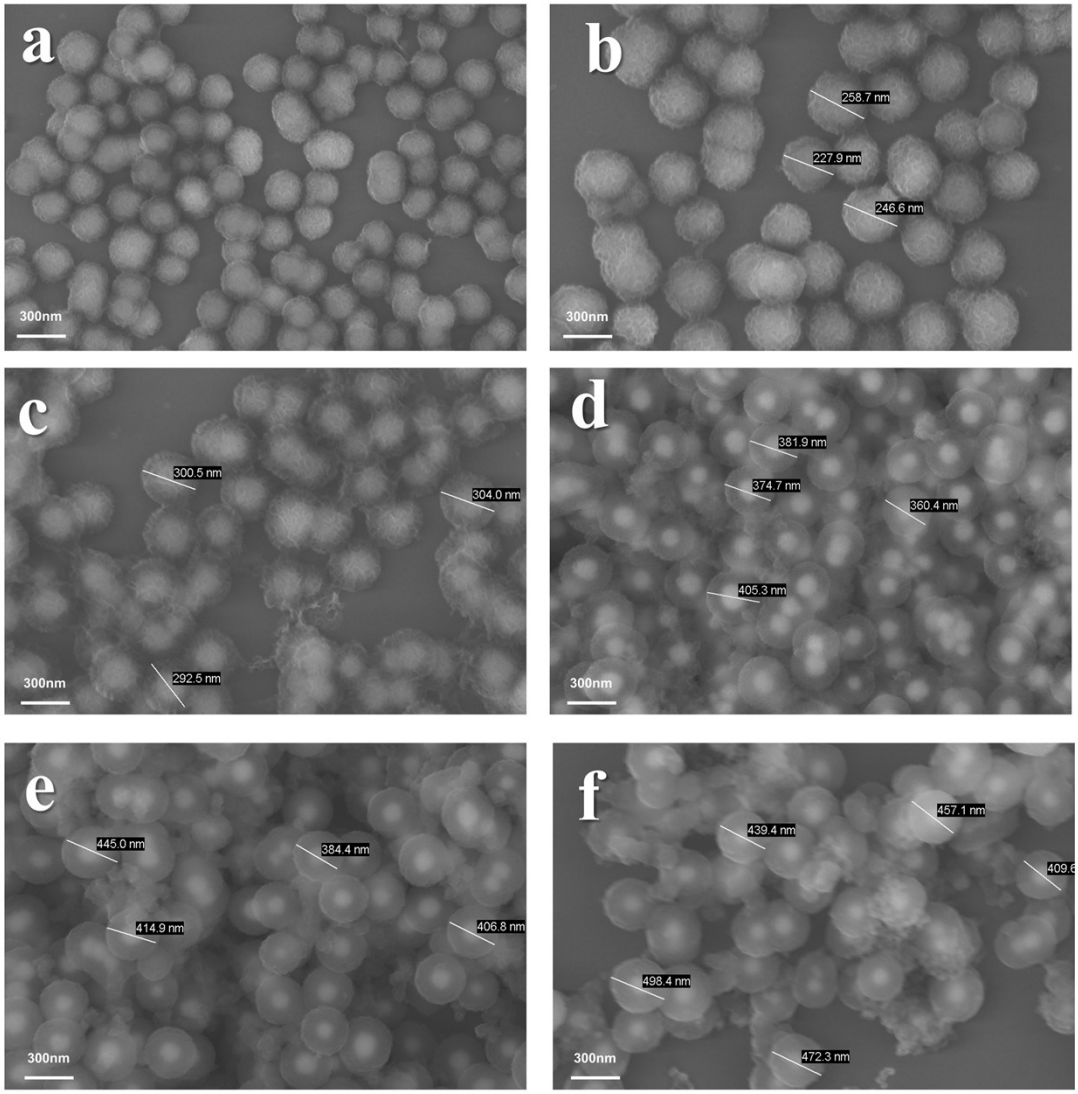

Figure S5. Morphological changes of FSDMS NPs at different reaction time a) 0 min, b) 5 min, C) 10 min, d) 20 min, e) 30 min, f) 45 min. A large number of secondary particles are formed after a long-time reaction.

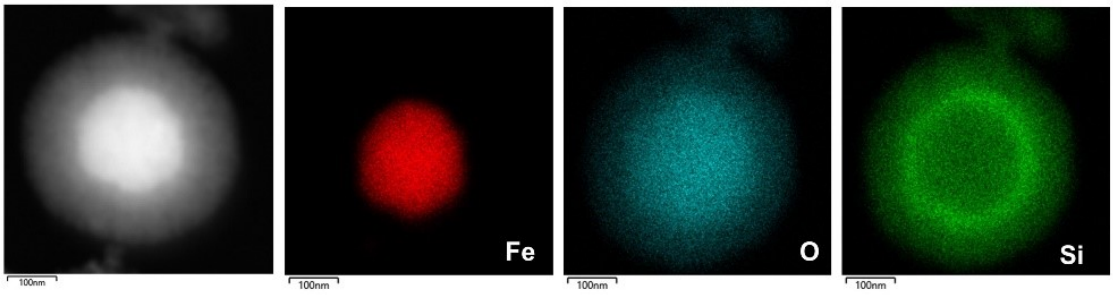

Figure S6. Element mapping image of FSDMS NPs. (Fe, O, Si) The center is composed of Fe_3O_4, and the outermost layer is free of Fe_3O_4, proving that there is no Fe_3O_4 load.

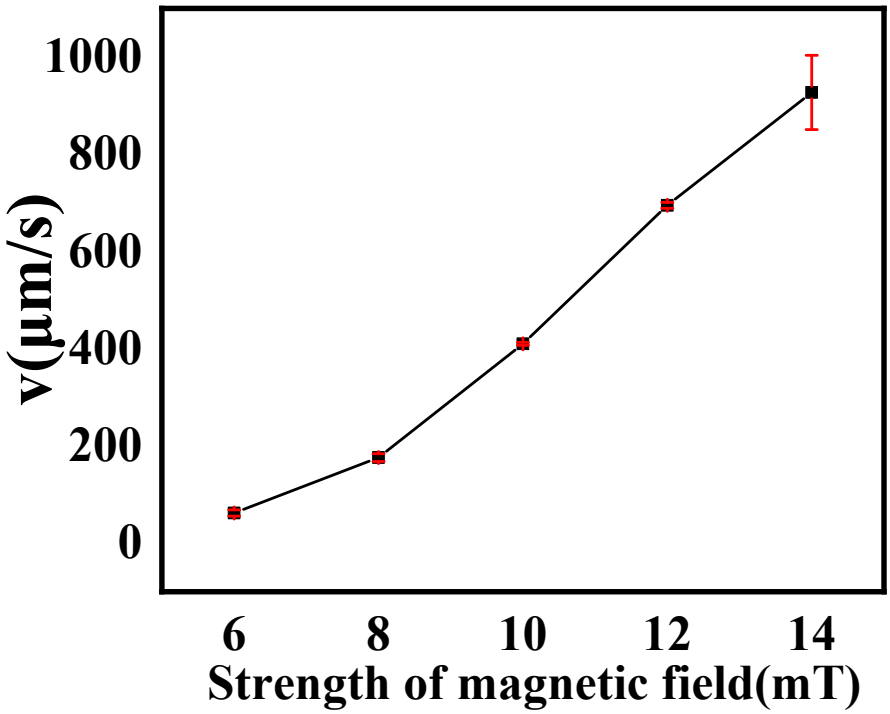

Figure S7. The effect of changing the magnetic field strength on the motion velocity of FSDMSsF NPs swarm: the velocity of the swarm increases with the increase of magnetic field intensity.

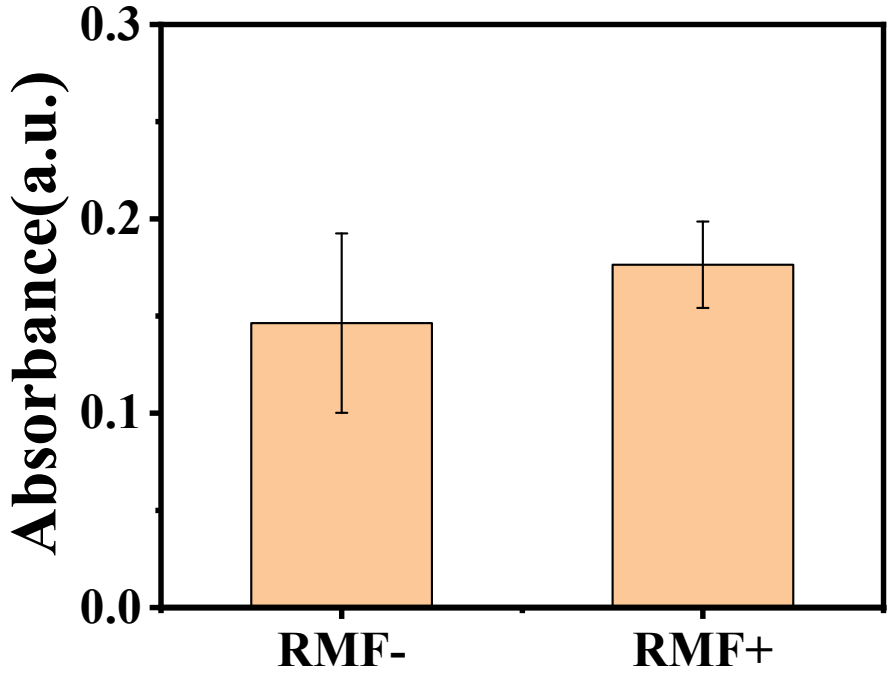

Figure S8. The absorbance of TMB oxidation catalyzed by FSDMSsF NPs with or without rotating magnetic field. (H_2O_2 10 mM, TMB 10 mg/mL, FSDMSsF NPs 200 μg/mL)

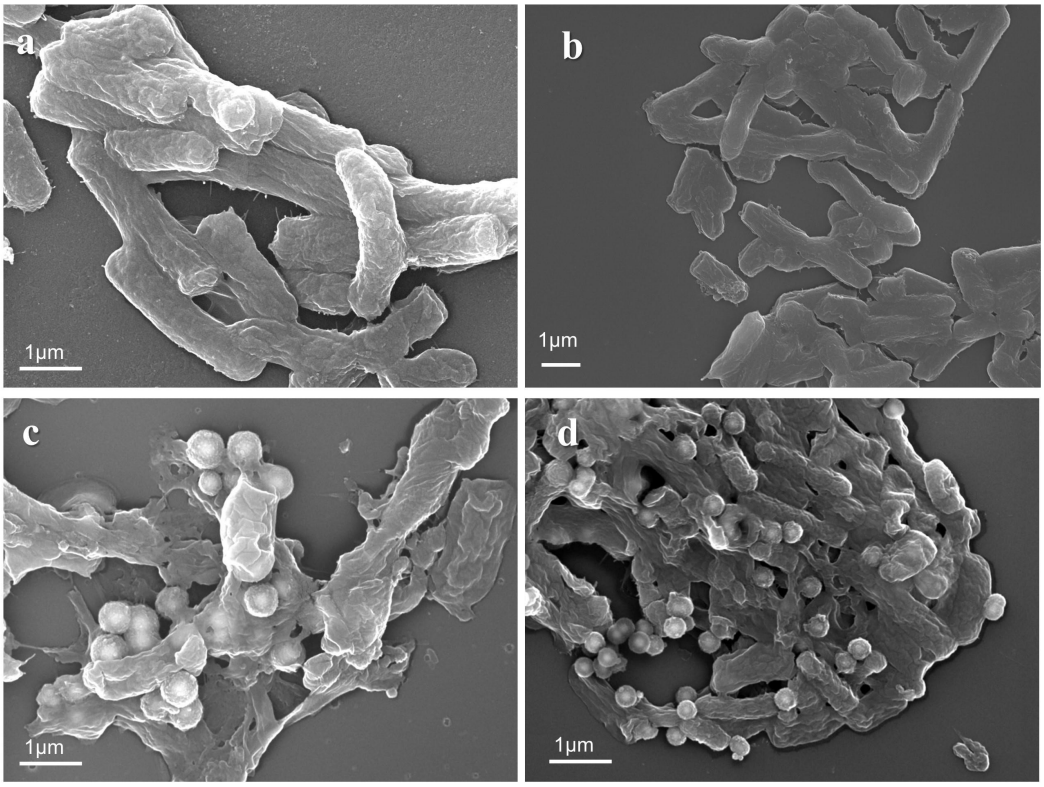

Figure S9. *E. coli* SEM images after magnetic field treatment: a) PBS, b) H_2O_2, c) FSDMSsF NPs, d) FSDMSsF NPs + H_2O_2.

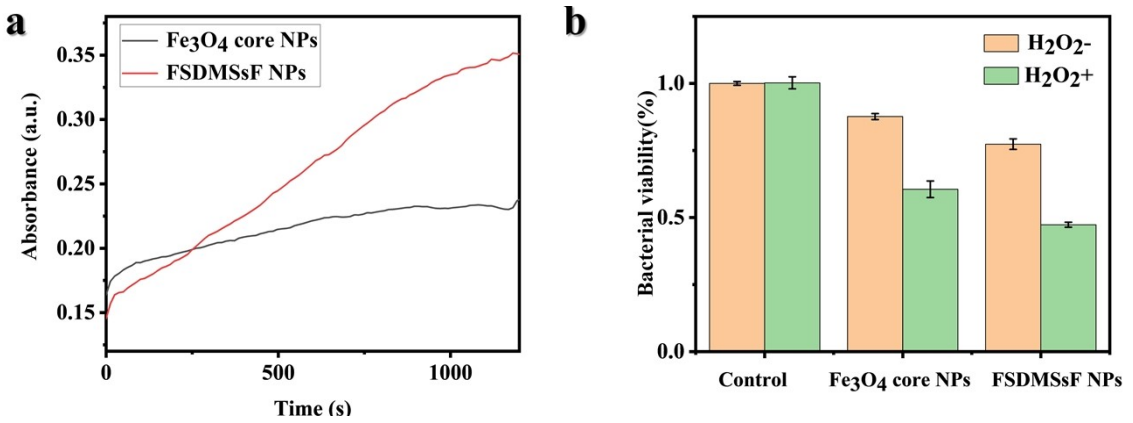

Figure S10. Comparison of catalytic performance between Fe_3O_4 core NPs and FSDMSsF NPs: a) Catalytic activity of Fe_3O_4 core NPs and FSDMSsF NPs (100 μg/ml). b) The relative activity of *E. coli* treated with Fe_3O_4 core NPs and FSDMSsF NPs. Error bars indicate standard deviation; the number n of parallel experiments is n = 3.

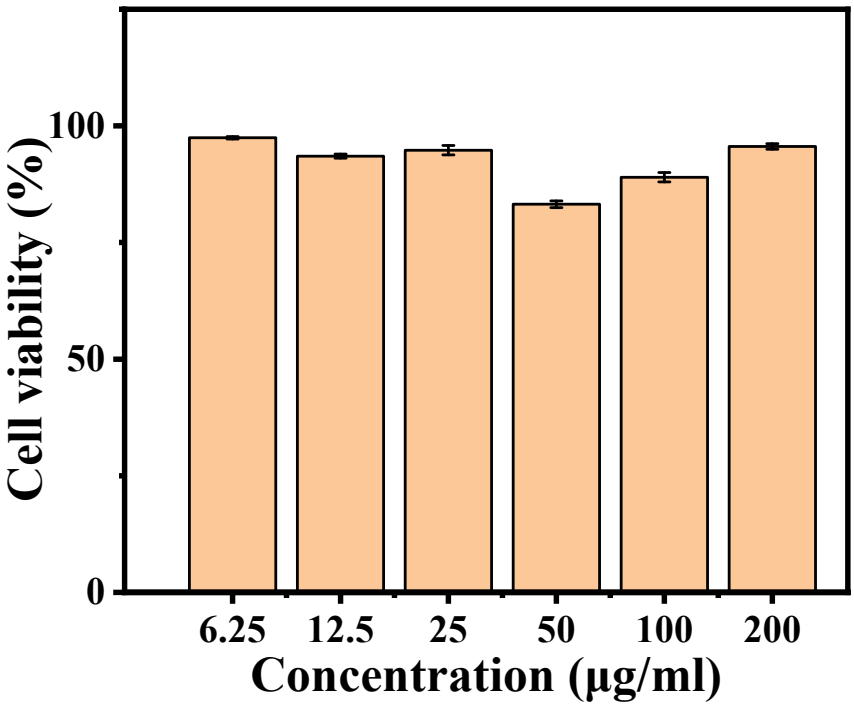

Figure S11. Cell viability of HEK-293T cells treated with different concentrations of FSDMSsF NPs solutions. Error bars indicate standard deviation; the number (n) of parallel experiments is n = 3.